第35卷 第2期 焊 接 学 报 Vol. 35 No. 2
2014年2月 TRANSACTIONS OF THE CHINA WELDING INSTITUTION February 2014

工艺参数对耦合 AA-TIG 焊电弧阳极电流密度的影响

黄 勇[1,2]， 王新鑫[2]， 瞿怀宇[2]， 樊 丁[1,2]
(1. 兰州理工大学 甘肃省有色金属新材料国家重点实验室，兰州 730050;
2. 兰州理工大学 有色金属材料先进加工成形技术教育部重点实验室，兰州 730050)

摘 要：针对耦合电弧 AA-TIG 焊，采用基于不锈钢阳极的钨探针法研究了主要工艺参数对电弧阳极电流密度分布的影响规律. 与常规 TIG 焊电弧相比，在相同条件下耦合 AA-TIG 焊电弧的阳极电流密度明显降低，并随着电弧电流和辅助电弧中氧气流量的减小以及钨极间距和弧长的增大而减小. 当主钨极和辅助钨极的间距较小时，耦合 AA-TIG 焊电弧的阳极电流密度符合高斯分布；当钨极间距较大时，阳极电流密度向双峰分布过渡，电弧边缘部位符合二次高斯分布，而中心部位偏离二次高斯分布.

关键词：AA-TIG 焊；耦合电弧；氧元素；阳极电流密度；探针法
中图分类号：TG404 **文献标识码**：A **文章编号**：0253-360X(2014)02-0005-05

0 序 言

钨极氩弧焊(TIG)是常规焊接方法中高质量焊接的代表，但受到钨极载流能力和电弧能量不够集中的限制，导致单道焊接熔深较浅，焊接效率较低，在一定程度上限制了它的应用. 活性 TIG 焊方法[1-4]通过在焊接过程中将活性元素引入到焊接电弧—熔池系统中，可使得熔深显著增加，不开坡口可焊透 8~12 mm 厚钢板，拓展了 TIG 焊的应用领域.

兰州理工大学[5,6]提出了一种新型的活性 TIG 焊方法，即电弧辅助活性焊(AA-TIG 焊，arc assisted activating TIG welding)方法，通过辅助电弧引入活性元素 O 可实现自动活性焊接. 该方法又分为两种模式，分别为分离电弧和耦合电弧模式. 耦合电弧 AA-TIG 焊中，辅助电弧为采用 $Ar+O_2$ 或 $Ar+CO_2$ 活性混合保护气体的小电流电弧，主电弧为正常工艺规范的氩电弧. 焊接时辅助电弧在前，主电弧在后，由于两者间距较小，形成耦合电弧，不但能显著增加熔深，而且还可以克服咬边和驼峰等成形缺陷，实现高速焊接[7].

文中采用基于水冷不锈钢阳极的探针法测量了耦合 AA-TIG 焊电弧的阳极电流密度分布，研究了焊接工艺参数对阳极电流密度的影响规律，这对于建立该方法的热源模型，研究其电弧特性变化的机理，揭示焊缝成形的机理，具有重要意义.

收稿日期：2012-11-12
基金项目：国家自然科学基金资助项目(51074084)；甘肃省自然科学基金资助项目(1010RJZA037)

1 试验方法

焊接电弧为耦合电弧 AA-TIG 定点焊的电弧，如图 1 所示，主电弧和辅助电弧都采用偏心铈钨极，间距为 2 mm，主电弧保护气体为 99.9 % 的氩气，辅助电弧保护气体为 $Ar+O_2$ 活性混合气体，阳极材料为水冷 SUS304 不锈钢. 分析了电弧电流、弧长、钨极间距、氧气流量等工艺参数对阳极电流密度分布的影响规律，基本工艺参数如表 1 所示.

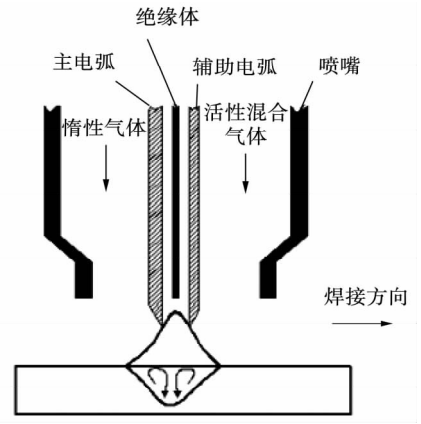

图 1 耦合电弧 AA-TIG 焊接示意图
Fig. 1 Schematic of coupling arc AA-TIG welding method

阳极电弧电流密度测量方法为钨探针法，试验装置如图 2 所示. 探针为直径 1 mm 钨极，采用刚玉管将其与水冷阳极不锈钢板隔开，保证钨探针与不锈钢阳极之间的良好绝缘，并采用水冷铜柱对钨探

表 1 耦合 AA-TIG 焊电弧的基础工艺参数

Table 1 Basic parameters of coupling AA-TIG arc

电弧种类	焊接电流 I/A	弧长 L/mm	钨极直径 D/mm	钨极角度 θ/(°)	保护气流量 Q/(L·min^{-1})
主电弧	50	3	3.2	30	25(Ar)
辅助电弧	30	3	2.4	30	23(Ar) +2(O_2)

针进行强制冷却. 阳极安装在移动精度为 0.01 mm 的轴滑台上,可实现阳极的二维平稳精确移动. 设定从主电弧钨极到辅助电弧钨极的连线为 x 轴正方向,两钨极尖端连线的中点为原点.

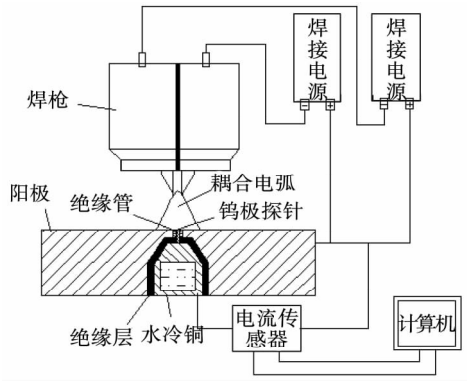

图 2 阳极电流密度测量系统

Fig. 2 Measuring system of arc anode current density

2 试验结果

2.1 电弧电流的影响

图 3 为不同电弧电流组合对耦合 AA-TIG 焊电弧阳极电流密度分布的影响规律. 随着电弧电流增大,电流密度峰值 J_{max} 增大,分布半径增大. 阳极电流密度峰值偏向于主电弧一侧,主电弧侧和辅助电弧侧的电流密度分布差别不明显.

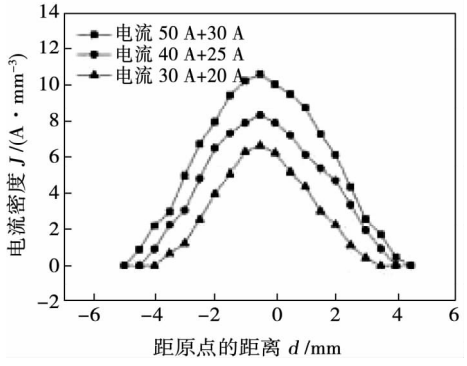

图 3 不同电弧电流组合对阳极电流密度分布的影响

Fig. 3 Effects of arc current on distribution of arc anode current density

图 4 为电流密度峰值随总电弧电流的变化规律. 随着总电弧电流的增大,电流密度峰值显著增大.

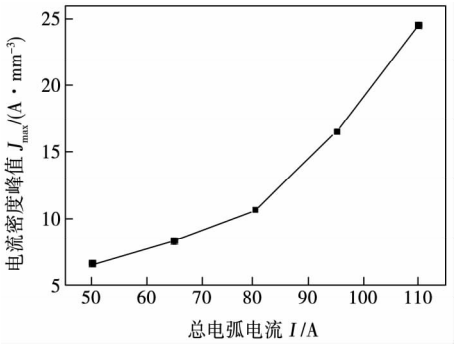

图 4 总电弧电流对阳极电流密度峰值的影响

Fig. 4 Effects of total arc current on peak value of arc anode current density

图 5 是耦合 AA-TIG 焊电弧与总电流下的 TIG 焊电弧和 TIG 焊主电弧的阳极电流密度分布的对比. 耦合 AA-TIG 焊电弧的阳极电流密度峰值和分布半径都介于总电流下的 TIG 电弧和 TIG 主电弧之间.

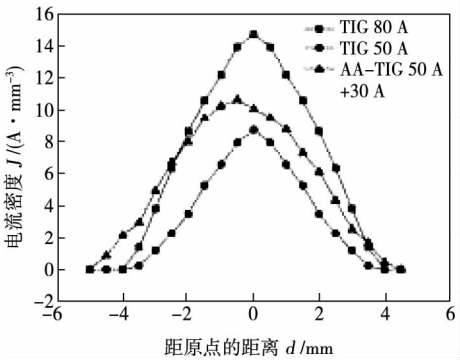

图 5 不同电弧对阳极电流密度分布的影响

Fig. 5 Effects of arc sort on distribution of arc anode current density

2.2 弧长的影响

图 6 所示为弧长对耦合 AA-TIG 焊电弧阳极电流密度分布的影响规律. 随着弧长增加,电流密度峰值大幅降低,其径向分布半径略有增大.

2.3 钨极间距的影响

图 7 为钨极间距 x 对耦合 AA-TIG 焊电弧阳极电流密度分布的影响规律. 随着主电弧和辅助电弧钨极间距的增大,耦合电弧电流密度峰值逐渐降低,电流分布作用范围增大. 当钨极间距增大到一定程度($x \geqslant 6$ mm) 时,电流密度的分布由一个峰值向两个峰值过渡,主电弧的电流密度峰值大于辅助电流的电流密度峰值.

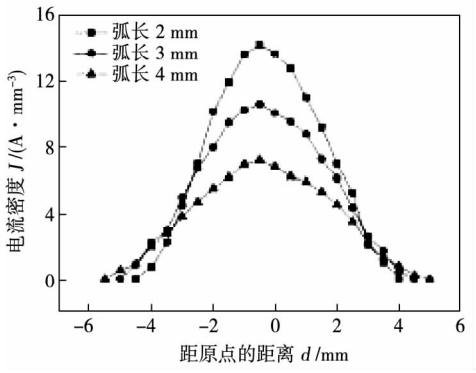

图 6　弧长对阳极电流密度分布的影响

Fig. 6　Effects of arc length on distribution of arc anode current density

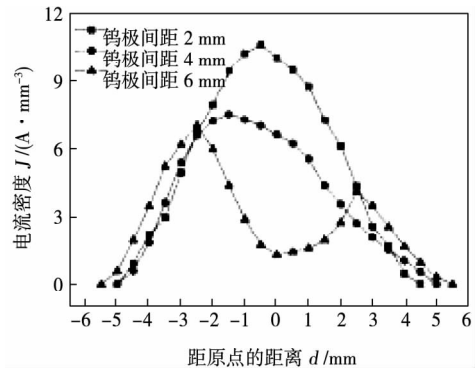

图 7　钨极间距对阳极电流密度分布的影响

Fig. 7　Effects of electrode spacing on distribution of arc anode current density

图 8 为阳极电流密度峰值随钨极间距的变化规律. 当钨极间距 x 很小($x=2$ mm) 时，主电弧和辅助电弧耦合作用很强，耦合电弧阳极电流密度峰值大于 TIG 焊主电弧的，但远小于总电流下的 TIG 焊电弧的. 随着钨极间距增大，耦合作用减弱，电流密度峰值呈

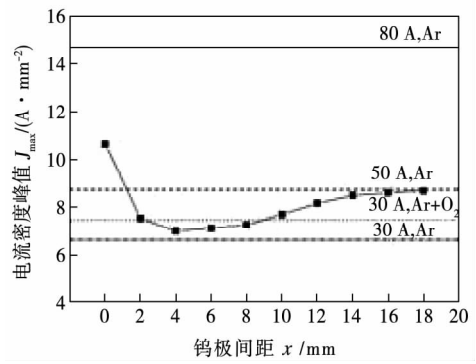

图 8　钨极间距对阳极电流密度峰值的影响

Fig. 8　Effects of electrode distance between main and assistant tungsten electrodes on peak value of arc anode current density

现先减小后增大的趋势，当 6 mm $\leqslant x \leqslant$ 10 mm 时达到最小值，该最小值介于辅助电弧(电流 30 A，保护气体为 Ar + O_2) 和同等电流 TIG 焊电弧(电流 30 A，保护气体为氩气) 的阳极电流密度峰值之间. 当钨极间距 $x \geqslant 6$ mm 时，随着钨极间距增大，主电弧与辅助电弧之间的耦合作用进一步减弱，电弧更多呈现单电弧的形貌，阳极电流密度峰值逐渐呈现为主电弧电流密度峰值. 当钨极间距 x 达到 20 mm 时，完全等于为主电弧电流密度峰值.

2.4　氧气流量的影响

当保持辅助电弧保护气体总流量一定时，随着活性混合气体中氧气流量的增加，阳极电流密度分布的变化规律如图 9 所示. 随着活性混合气体中氧气流量的增加，阳极电流密度峰值略有增大，而分布范围没有明显变化.

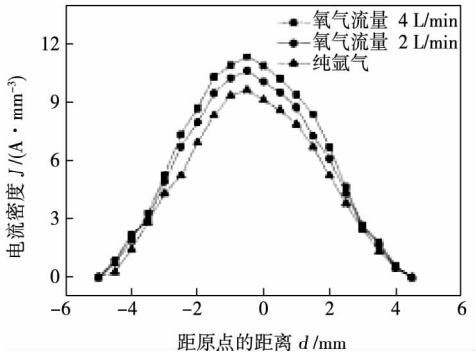

图 9　氧气流量对阳极电流密度分布的影响

Fig. 9　Effects of oxygen flow rate on distribution of arc anode current density

3　分析与讨论

对于耦合 AA-TIG 焊电弧，存在着耦合电弧和活性元素 O 引入对其电弧特性的影响. 从试验结果来看，包括电弧电流、弧长和电极间距等耦合电弧工艺参数对其电流密度分布的影响较大，而通过辅助电弧保护气体中的氧气引入活性元素 O，虽然由于氧气解离对电弧的冷却作用在一定程度上收缩了电弧，但从电流密度分布的变化来看，这种收缩作用并不是很明显.

关于耦合电弧对耦合 AA-TIG 焊电弧阳极电流密度的影响，由图 10 可知，由于主电弧和辅助电弧之间电磁场的相互吸引作用，电弧将偏离原来的轴向方向，向对方倾斜，从而使得耦合电弧阳极电流密度峰值 J_{max} 小于主电弧的，分布半径增大. 电弧电流、弧长和钨极间距都对电流密度峰值和分布半径

有明显影响,尤其是钨极间距,还将影响电流密度分布形态. 从图 7 和图 8 可知,当钨极间距 x 从 2 mm 向 20 mm 变化时,由于两电弧之间相互吸引作用减弱,电流密度分布曲线将由单峰向双峰曲线转变,电弧也从一个统一的耦合电弧向两个独立的分离电弧过渡,这与 Ogino 等人[8]的研究相一致.

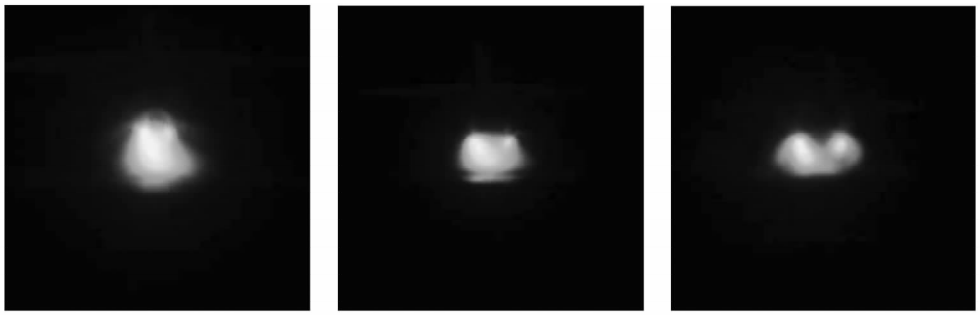

(a) 2 mm 钨极间距 (b) 4 mm 钨极间距 (c) 6 mm 钨极间距

图 10 不同钨极间距时的电弧形貌

Fig. 10 Arc appearances at different electrode spacing

图 11 为不同钨极间距下的耦合 AA-TIG 焊电弧阳极电流密度试验值和高斯拟合曲线. 当钨极间距较小($x \leqslant 4$ mm)时,阳极电流密度分布完全符合高斯分布. 而当间距较大($x > 4$ mm)时,电弧边缘部位的阳极电流密度分布基本符合二次高斯曲线,但电弧中间部位偏离于二次高斯分布曲线,试验值略大于拟合值. 在主电弧侧,偏离不明显,而在辅助电弧侧偏离较明显. 二次高斯曲线两峰值的间距略小于主电弧和辅助电弧的钨极间距. 这些都是由于主电弧和辅助电弧之间的相互吸引所形成的电弧偏转作用导致的,由于辅助电弧电流较小,电弧挺直性较弱,电弧偏离于原始高斯曲线分布较明显.

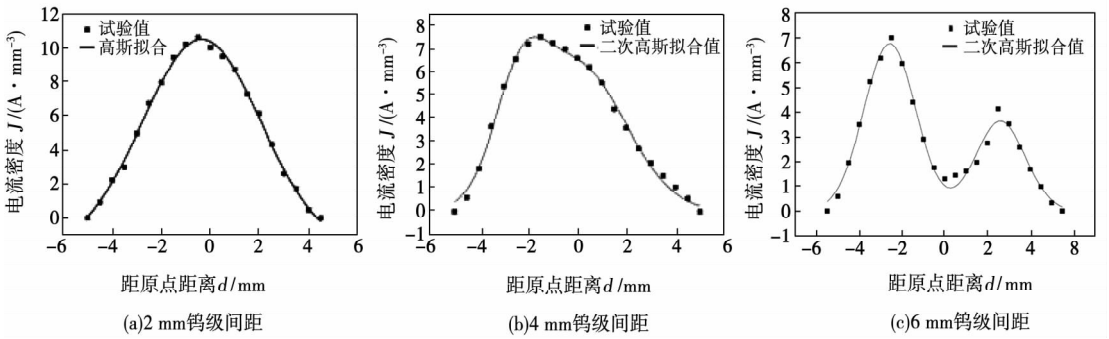

图 11 不同钨极间距时的阳极电流密度分布高斯拟合

Fig. 11 Gaussian fittings of arc anode current density distribution at different electrode spacing

4 结 论

(1) 与 TIG 焊电弧相比,在相同条件下耦合 AA-TIG 焊电弧的阳极电流密度明显降低,并随电弧电流的减小、弧长的增大、钨极间距的增大、辅助电弧中氧气流量的减小而减小.

(2) 当主钨极和辅助钨极的间距较小时,耦合 AA-TIG 焊电弧的阳极电流密度符合高斯分布,当钨极间距较大时,阳极电流密度向双峰分布过渡,电弧边缘部位符合二次高斯分布,而中心部位偏离二次高斯分布.

(3) 电弧电流、弧长和钨极间距等耦合电弧工艺参数对耦合 AA-TIG 电弧阳极电流密度分布影响较大,而 O 元素引入的影响较小.

参考文献:

[1] Paton B E. Contraction of the welding arc caused by the flux in tungsten-electrode argon arc welding [J]. The Paton Welding Journal, 2000(1): 5-11.

[2] Paskell T, Lundin C. GTAW flux increases weld joint penetration

[1]. Welding Journal, 1997, 76(4): 57 - 62.

[3] Huang Y, Fan D, Shao F. Alternative current flux zoned tungsten inert gas welding process for aluminium alloys [J]. Science and Technology of Welding and Joining, 2012, 17(2): 122 - 127.

[4] 陆善平, 董文超, 李殿中, 等. 不锈钢材料的高效焊接新工艺 [J]. 金属学报, 2010, 46(11): 1347 - 1364.
Lu Shanping, Dong Wenchao, Li Dianzhong, *et al*. High efficiency welding process for stainless steel materials [J]. Acta Metallurgica Sinica, 2010, 46(10): 1347 - 1364.

[5] 樊　丁, 林　涛, 黄　勇, 等. 电弧辅助活性 TIG 焊接法 [J]. 焊接学报, 2008, 29(12): 1 - 4.
Fan Ding, Lin Tao, Huang Yong, *et al*. Arc assisted activating TIG welding process [J]. Transactions of the China Welding Institution, 2008, 29(12): 1 - 4.

[6] 黄　勇, 樊　丁, 林　涛, 等. 不锈钢电弧辅助活性 TIG 焊 [J]. 焊接学报. 2009, 30(10): 1 - 4.
Huang Yong, Fan Ding, Lin Tao, *et al*. Arc assisted activation TIG welding process for stainless steels [J]. Transactions of the China Welding Institution, 2009, 30(10): 1 - 4.

[7] 杨　磊, 樊　丁, 黄　勇, 等. 耦合电弧 AA-TIG 高速焊工艺 [J]. 电焊机, 2011, 41(5): 57 - 61.
Yang Lei, Fan Ding, Huang Yong, *et al*. Research on coupling arc AA-TIG high speed welding process [J]. Electric Welding Machine, 2011, 41(5): 57 - 61.

[8] Ogino Y, Hirata Y, Nomura K. Numerical analysis of the heat source characteristics of a two-electrode TIG arc [J]. Journal of Physics D: Applied Physics, 2011, 44(6): 1 - 7.

作者简介: 黄　勇,男,1972 年出生,博士,副教授. 主要从事高效焊接技术研究. 发表论文 40 余篇. Email: hyorhot@lut.cn

MAIN TOPICS, ABSTRACTS & KEY WORDS

New magnetic bias suppression method for full bridge inverters DUAN Bin, ZHANG Chenghui, SUN Tongjing, ZHANG Guangxian (School of Control Science and Engineering, Shandong University, Jinan 250061, China). pp 1 – 4

Abstract: To overcome the magnetic bias and low reliability of conventional the full bridge inverter, a magnetic bias real-time detection and suppression method is proposed. The method combines advantages of the analog detection and digital control, in which the transformer primary current and the output current are acquired simultaneously to participate the dynamic control process. The detection system can output the moment and strength of the magnetic bias signal in real time, by which the digital controller can adjust PWM driving pulses and ensure that the system can quickly and effectively suppress magnetic bias. Experimental results show that the proposed method has good consistency, versatility, stability and high reliability, which can be widely used in the system composed of full bridge inverters.

Key words: full bridge inverter; magnetic bias; high power source; reliability

Effects of arc parameters on arc anode current density of coupling AA-TIG arc HUANG Yong[1,2], WANG Xinxin[2], QU Huaiyu[2], FAN Ding[1,2] (1. State Key Laboratory of Gansu Advanced Non-ferrous Metal Materials, Lanzhou University of Technology, Lanzhou 730050, China; 2. Key Laboratory of Non-ferrous Metal Alloys, The Ministry of Education, Lanzhou University of Technology, Lanzhou 730050, China). pp 5 – 9

Abstract: Influences of main process parameters on arc anode current density distribution of coupling arc AA-TIG welding were analyzed, using the tungsten probe measurement based on stainless steel anode. Compared with normal TIG arc, the anode current density of coupling AA-TIG arc is obviously lower in the same condition. It is decreased with the increase of arc current and oxygen flowrate in the assisted arc, the decrease of tungsten electrode spacing and arc length. When the spacing between the main electrode and assisted electrode is small, the distribution of arc anode current density fits a Gaussian profile. When the electrode spacing is large, it gradually turns to a bimodal distribution. The anode current density at the arc edge is consistent with a quadratic Gaussian distribution, while that at the middle region between the main arc and assisted arc deviates from the quadratic Gaussian distribution.

Key words: AA-TIG welding; coupling arc; oxygen element; anode current density; probe measurement

Automatic welding machine system designed for titanium alloy tube-sheet joint of power plant condenser WANG Zhenmin, PAN Chengrong, FENG Yunliang, QUE Fuheng (School of Mechanical & Automotive Engineering, South China University of Technology, Guangzhou 510640, China). pp 10 – 14

Abstract: To improve the welding quality of circumferential welds of the titanium tube-sheet joint of power plant condenser, an automatic tube-sheet welding system with digital control and visual operation characteristics is developed. The main circuit of welding inverter adopted a frequency of 100 kHz full-bridge topology for improving the dynamic response performance. The digital control system for the welding process is designed based on ARM Cortex-M4, in which the LM4F232 MCU is used as the core element. The parameter self-tuning PI algorithm based on fuzzy logic judge is developed to improve the welding adaptability under different working conditions. The human-computer interactive system based on ARM microprocessor and touch screen is designed, achieving digitalization and visualization of human-computer interaction. System testing and welding experiments show that the developed tube sheet automatic welding machine is with good performance, and can meet the demands of high quality and efficiency welding for the condenser titanium tube sheet joints.

Key words: titanium alloy tube sheet; digital control; visual operation; tube sheet welding machine

Low temperature sintering-bonding and the performance of joints using Ag_2O paste with an adding of Ag-coated Cu particles ZHAO Zhenyu[1], MU Fengwen[1], ZOU Guisheng[1], LIU Lei[1*], YAN Jiuchun[2] (1. Department of Mechanical Engineering, Tsinghua University, Beijing 100084, China; 2. State Key Laboratory of Advanced Welding & Joining, Harbin Institute of Technology, Harbin 150001, China). pp 15 – 18

Abstract: The micro-scaled Ag_2O paste is cheaper than Ag nanoparticle paste and has a promising application prospect in high temperature electronic packaging industry. In order to further reduce the cost and improve the joint ability of the resistance to electrochemical migration (ECM), the Ag-coated Cu particles were added into the original micro-scaled Ag_2O paste to make a new composite paste. In this paper, the shear strength of joints obtained by using the original Ag_2O paste and the new Ag_2O paste contained Ag-coated Cu particles and the two sintered pastes´ability of resistance to ECM were compared. The results revealed that the average shear strength of joints obtained by using the new Ag_2O paste with Ag-coated copper at the typical bonding condition (250 ℃, 5 min, 2 MPa) showed an obvious decrease, while the ability of the resistance to ECM got a significant increase due to the addition of Ag-coated Cu particles.

Key words: Ag-coated Cu particles; Ag_2O paste; Electrochemical migration (ECM); Electronic packaging